Comparison of Model- and Full-Scale Wind-Tunnel Performance

Brian E. Smith* and Peter T. Zell†
NASA Ames Research Center, Moffett Field, California
and
Patrick M. Shinoda‡
U.S. Army Aviation and Technology Activity-AVSCOM
Moffett Field, California

Experimental results from the Integrated Systems Test of the upgraded National Full-Scale Aerodynamics Complex 40- by 80-ft wind tunnel located at NASA Ames Research Center, which took place in 1987, are compared with results obtained with a 1/50 scale model of the wind tunnel. Test-section flow characteristics, air-exchange performance, total pressure distributions, and wall-static pressure distributions obtained with the model- and full-scale facilities are compared. The 1/50-scale model data were used to predict qualitative performance trends of the full-scale facility during investigation of design changes. Despite large differences in scale and Reynolds number between the two tunnels, quantitative agreement between certain model and full-scale performance characteristics was quite good.

Nomenclature

C_p = pressure coefficient
p = pressure
q = dynamic pressure, $\rho U^2/2$
Re = Reynolds number
T = temperature, °F
U = freestream velocity
u = velocity component in x direction
u' = velocity fluctuation in x direction
w = width
x = longitudinal coordinate
y = horizontal coordinate
z = vertical coordinate

Subscripts
a = atmosphere
avg = average
cr = critical
mean = mean
s = static
t = total
ts = test section

Introduction

IN support of the upgrade of the NASA Ames 40- by 80-ft wind tunnel, a series of investigations was carried out using a 1/50-scale model of the facility. It was expected that the aerodynamic characteristics of a small-scale model would give a reliable qualitative indication of the performance of the full-scale facility. Because of the large differences in scale and Reynolds number between the model- and full-scale tunnels, the quantitative results obtained at model scale were not necessarily expected to duplicate the actual performance of the full-scale wind tunnel. This article will present comparisons of full-scale measurements made during the 1986 Integrated Systems Test (IST) of the 40- by 80-ft wind tunnel with data obtained in the 1/50-scale studies.

The upgrade of the Ames 40- by 80-ft wind tunnel was intended to increase the airspeed in the 40- by 80-ft test section and to add a much larger test section to the wind-tunnel complex.[1] The reason for the modification was the need to test evolving V/STOL aircraft at full-scale speeds and Reynolds numbers. The modifications consist of an increase in tunnel-drive power from 36,000 to 125,000 hp, the addition of an acoustic liner within the 40- by 80-ft test section, the installation of new turning vanes and an air-exchange system, and the addition of a nonreturn leg that has an 80-ft by 120-ft test section. The principle features of the 40- by 80- by 120-ft wind tunnel, which is part of the National Full Scale Aerodynamics Complex (NFAC), are shown in Fig. 1.

In order to provide estimates of the performance of the full-scale wind tunnel in the modified configuration, a 1/50-scale model of the facility was constructed. The model simulated the various aerodynamic features slated for upgrade and/or modification as well as those elements in the circuit, which would remain unchanged. A model 1/50th the scale of the full-scale facility could be constructed with the proper geometry (i.e., number of turning vanes arranged with accurate chord-to-gap ratios) without resorting to exotic materials or techniques. On the other hand, the model had to be small enough to satisfy the budgetary and schedule constraints of the wind-tunnel modification project. Where it was felt that larger scale was necessary to increase the fidelity and confidence in the measurements, component tests were carried out at up to 1/10th scale.[1]

The principle aerodynamic features of the full-scale wind tunnel are replicated in the model, i.e., turning vane configuration, number of fan drive motors, etc. The internal shapes of the various components were scaled properly, and considerable care was taken to simulate the aerodynamics loss characteristics of the major elements within the circuit. However, for practical reasons, it was not possible to duplicate at small scale

Presented as Paper 88-2536 at the AIAA 6th Applied Aerodynamics Conference, Williamsburg, VA, June 6-8, 1988; received Nov. 25, 1988; revision received June 16, 1989.

*Aerospace Engineer. Member AIAA.
†Aerospace Engineer.
‡Aerospace Engineer, Aeroflightdynamics Directorate.

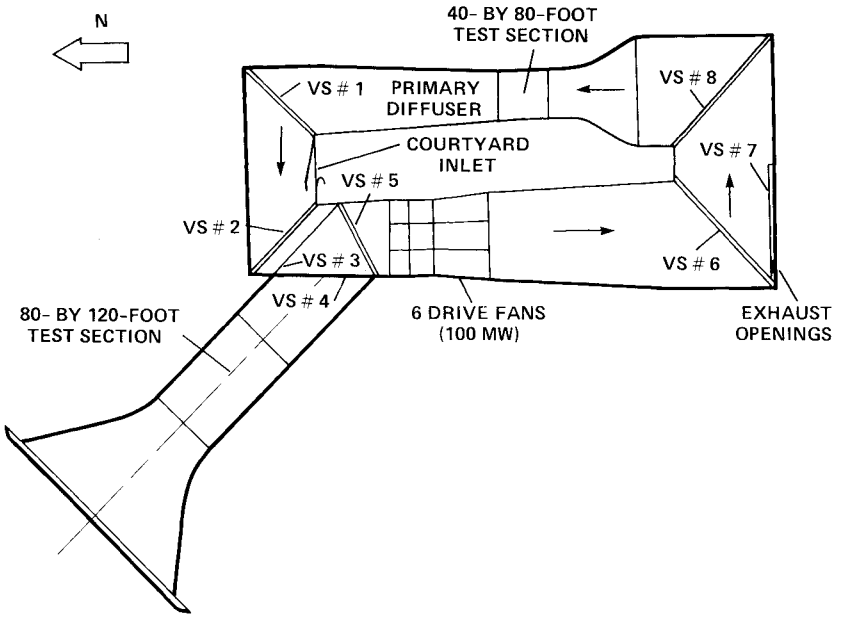

Fig. 1 Planview of NFAC located at Ames Research Center, which illustrates 40- by 80-ft and 80- by 120-ft wind-tunnel circuits.

Table 1 Comparison of the characteristics of the full-scale and model-scale turning vanes

	Chord, ft		Local velocity, ft/s		Chord Reynolds number	
Vane set	Full scale	1/50th scale	Full scale	1/50th scale	Full scale	1/50th scale
1	6.0	0.12	169	84.0	6.4×10^6	6.3×10^4
2	6.0	0.12	186	92.4	7.0×10^6	6.9×10^4
6	17.2	0.34	58.6	29.2	6.3×10^6	6.3×10^4
8	3.0	0.06	53.2	26.5	1.0×10^6	9.9×10^3

certain features of the larger wind tunnel such as the corrugated wall cladding and fastener details. The model was constructed primarily of molded fiberglass, wood, and clear Lucite panels. The latter material was used to permit observation of tufts and other flow-visualization media.

Though every effort was made to configure the model to represent the full-scale wind tunnel accurately, significant aerodynamic differences exist between the model- and full-scale fan drive sections. Both wind tunnels are powered by a bank of six fan motors, each of which is situated within its own nacelle. The full-scale fans have 15 blades and 23 stators per fan and have a solidity of 56%.[2] The fans in the model each have six blades and seven stators with a solidity of 31%.[3] When looking upstream, the full-scale fans rotate clockwise, which is opposite to the rotational direction of the model-scale fans. The full-scale fan blades have variable-pitch capability, whereas the model-scale fan blades are fixed pitch. Because the full-scale fan motors are synchronized at the frequency of the power system, their rotational speeds are identical. In contrast, the 1/50-scale fan motors, though equally powered, are not constrained to rotate at the same speed. Differences in rotational speeds of up to several percent were measured among the model-scale fans.

The corner turning vane sets in the model were constructed of shaped hardwood. The airfoil sections, sizes, and chord-to-gap ratios were scaled to represent the full-scale vanes properly. Table 1 presents a comparison of the characteristics of the full-scale and model-scale turning vanes.[4] The large differences in Reynolds number between the full- and model-scale turning vanes contributed to some uncertainty in the results, especially in the comparisons of the static pressure distribution within the circuit. The Reynolds number of the model-scale turning values were all well below the critical Reynolds number Re_{cr}. For this reason, it was expected that the drag of the 1/50-scale turning vanes would be greater than the full-scale vanes.

Maximum airspeed in the 40- by 80-ft test section of the full-scale facility is 300 knots ($q_{ts} = 262$ lb/ft^2). In contrast, the maximum airspeed in the 0.8- by 1.2-ft test section of the model is only 137 knots ($q_{ts} = 62$ lb/ft^2). Lining the test section of the full-scale tunnel is a 6-in.-thick layer of acoustically absorbent material designed to attenuate reflections of sound. This lining is aerodynamically but not acoustically simulated in the model test section by the addition of a 0.12-in. layer of fiberglass.

The remainder of this article will describe the instrumentation used for the model- and full-scale investigations. Comparisons of test section flow quality and temperature measurements, air-exchange performance, and surveys of pressure made at various locations in the two facilities will then be presented.

Experimental Instrumentation

All pressure measurements in the 1/50-scale model were made using an electronically scanned pressure measurement system under the control of a microcomputer. This hardware enabled simultaneous measurement of all total and static pressures on the model. In most cases, 60 measurement samples were obtained over a time period of 1s to produce an ensemble-averaged data point. The full-scale range of the transducers used for the model-scale measurements was 5 lb/in.^{2}. The end-to-end accuracy of the pressure measurement system was $\pm 0.1\%$ of the full-scale range. Lateral total pressure surveys of the flowfield inside the model were made using a single Kiel probe in the test section and eight probe rakes at other locations in the model. The probes were positioned by a stepper controller, which was also driven by the microcomputer system. A complete lateral survey at a given location in the model could thus be performed automatically under computer control. Time-averaged measurements of wall static pressures referenced to atmospheric were made simultaneously at over 130 locations around the model.

The lateral distribution of axial turbulence intensity, $\sqrt{\overline{u'^2}}/U$ in the 1/50-scale test section was made using a single hot wire. It has been shown that a single wire oriented normal to the mean-flow direction is sensitive only to u' for flows in which the mean axial velocity is large relative to the three fluctuating velocity components.[5] The hot-wire probe was positioned with the same traverse rig used to drive the total pressure Kiel probe. The fluctuating voltage signal from the anemometer electronics connected to the sensing element was recorded on the x-y plotter together with the position signal from a potentiometer on the traverse mechanism. Total temperature surveys in the test section of the model were made using a thermocouple on a motor-controlled traverse rig.

Measurements of the volume rate of flow into the air-exchange inlet of the model were made using a commercially available balometer.[6] The instrument measures air flow by mechanically integrating the total and static pressure differential across a grid of known size through which the air flows. The accuracy of the balometer is estimated to be ± 3%.

Since the 40- by 80-ft wind tunnel IST was an evaluation of the wind-tunnel performance as well as a test of the ancillary systems, a large number of aerodynamic, structural, and electrical measurements were made. The extensive amount of aerodynamic instrumentation provided a unique opportunity for comparison with data from the detailed measurements made in the 1/50-scale model.

During the IST, measurements of flow quality in the test section were made at midheight or 19.5 ft above the floor of the test section.[7] The flow quality sensors were located at the longitudinal center of the test section. Measurements of the lateral distribution of total and static pressure were made using fixed, Pitot-static probes mounted at 10-ft increments along a horizontal line in the test section. Collocated with the Pitot-static probes were total temperature thermocouples and single hot wires. A cross wire was mounted on the center of the instrumentation boom in order to obtain measurements of turbulence intensity in the lateral direction. The probes spanned the central 75% of the test section width. In the model, the survey line was located at the vertical center of the test section approximately 10% of test section length upstream of the midpoint of the test section. The pressure data in the test section of the full-scale wind tunnel were obtained using the same electronically scanned pressure measurement system used for the model scale tests.

In the full-scale tests, measurements of the total and static pressure in the flowfield upstream of the turning vanes were made with Pitot-static probes affixed to supports, which projected approximately one chord length upstream of the airfoil leading edges. Mechanical pressure scanners and/or individual transducers were used to measure the pressure signals from these probes depending on the expected range of pressures. At approximately 80 locations along the center of the wind-tunnel ceiling, time-averaged static pressure measurements were made using mechanical pressure scanners.

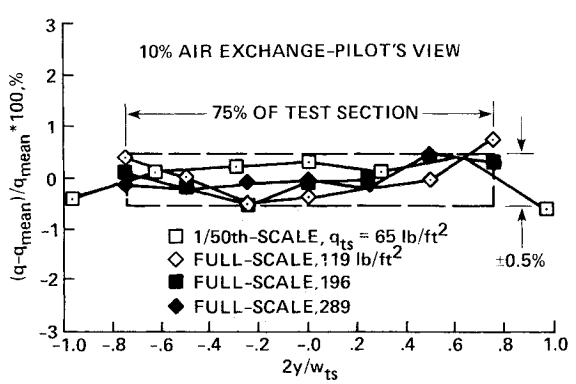

Fig. 2 Comparisons of lateral distributions of dynamic pressure measured at midheight in test sections of 1/50- and full-scale wind tunnels.

Results and Discussion

Two-Section Flow Quality

Of primary interest in the model-scale investigations was the effect on test-section flow quality of various modifications to elements of the wind-tunnel circuit. Changes in the turning characteristics of the vane sets upstream of the test section and alterations to the air-exchange inlet and exhaust configurations were expected to affect the flow uniformity of the 1/50-scale section to a sufficient degree that qualitative trends would be evident.

A comparison of the lateral variation of dynamic pressure as a percent of the mean value across the test sections in the 1/50-scale and full-scale test sections for an air-exchange rate of 10% is shown in Fig. 2. The small-scale data are shown for a test section dynamic pressure of 65 lb/ft². The full-scale measurements were made at test-section dynamic pressures of 119, 196, and 289 lb/ft². The flow-quality specification of less than ± 0.5% variation from the mean over the central 75% of the test section is also shown in the figure. The lateral variation of dynamic pressure measured in the model meets the flow-quality specification over virtually the entire test-section width. The lateral distribution measured in the full-scale facility satisfies the flow-quality specification for all but the lowest test-section dynamic pressure level. This may be partially due to the fact that at low levels of test-section dynamic pressure, the measurement uncertainty in the full-scale data is larger.

It is important to note that the full-scale pressure data were obtained simultaneously at all lateral locations in the test section. In contrast, the small-scale data were obtained by means of a spacial traverse, which required approximately 30 s. Because of this, spacial variations in the pressure distribution are intermingled with time variations in tunnel pressure and velocity levels. Despite this fact, the lateral distributions of dynamic pressure obtained at model scale were very repeatable. This would indicate that the flow within the 1/50-scale facility was stable for a given fan speed.

A comparison is presented in Fig. 3 of the lateral distribution of axial turbulence intensity in the model- and full-scale test sections. The design goal for the turbulence intensity in the axial direction ($\sqrt{\overline{u'^2}}/U$ *100 = 0.5% over the central 75% of the test section width) is shown in the figure. The agreement is quite good between the model- and full-scale measurements of axial turbulence intensity. This result is noteworthy considering the different characteristics of the model- and full-scale fan drive sections and the large differences in Reynolds number between the model- and full-scale turning vanes, which are located upstream of the test section. It was observed that the distribution of turbulence intensity in the test section of the model was sensitive to changes in aerodynamic components elsewhere in the circuit and was thus a reliable indicator of the consequences of the changes.

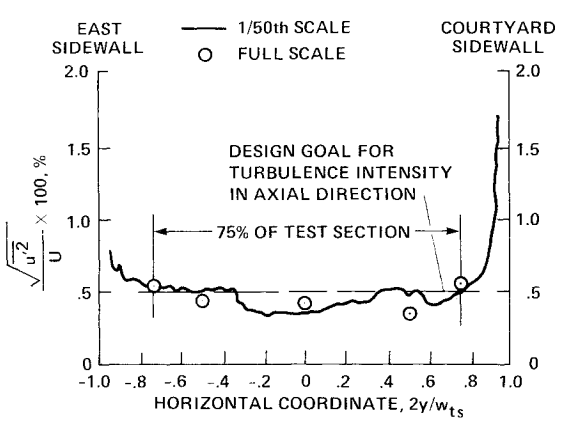

Fig. 3 Comparison of lateral distributions of turbulence intensity measured at midheight in test sections of 1/50- and full-scale wind tunnels.

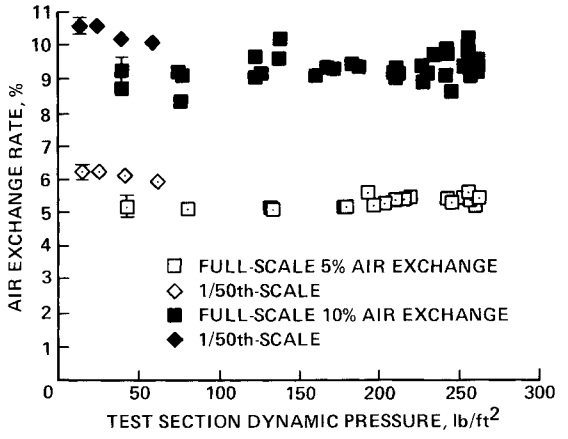

Fig. 4 Comparisons of air-exchange rate vs test-section dynamic pressure for inlet door positions corresponding to full-scale openings of 5 and 10 ft, respectively.

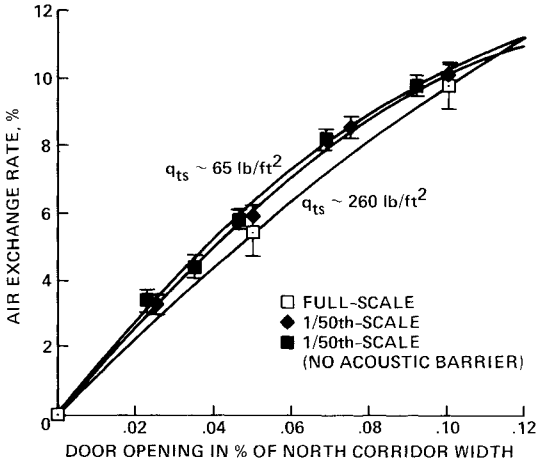

Fig. 5 Comparisons of air-exchange rate vs inlet door position.

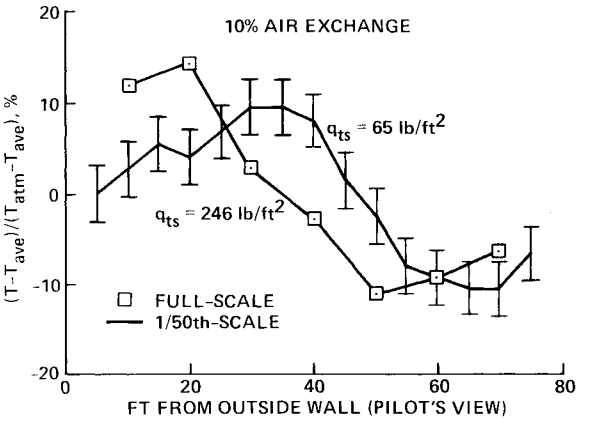

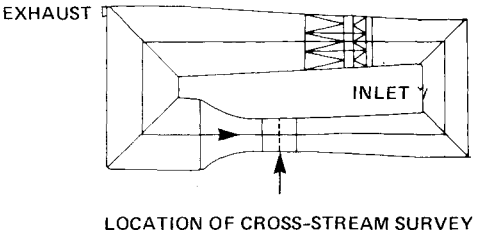

Fig. 6 Comparisons of lateral distributions of total temperature measured at midheight in test sections of 1/50- and full-scale wind tunnels.

Air-Exchange System Performance

The model tunnel was also used to assess the performance of the redesigned, full-scale, air-exchange system.[7] In particular, the model was used to determine the changes in air-exchange effectiveness as the configurations of the inlet and exhaust were changed. In addition, the lateral distribution of total temperature in the test section was measured in order to determine the effect of the locations at which air is admitted to and expelled from the circuit. The full-scale facility incorporates an air inlet design that admits air tangentially along the inner wall of the wind tunnel in the high-speed or north end. The air-exchange inlet (and exhaust) of the 1/50-scale model was configured with screens and aluminum bars to approximate the total pressure loss through the full-scale inlet structure.

A comparison of the air-exchange rates for the model- and full-scale facilities as a function of test-section dynamic pressure is presented in Fig. 4. Data from two different inlet door positions are presented corresponding to nominal air-exchange rates of 5 and 10%, respectively. The model-scale data are presented over a range of test-section dynamic pressures from 14 to 65 lb/ft^2. The full-scale data are shown over a range of dynamic pressures up to the maximum of 262 lb/ft^2. Some overlap in the model- and full-scale dynamic pressure ranges was possible. The error bars shown represent uncertainty in the calculation of the air-exchange rates. The air-exchange rates measured in the model are slightly higher than the rates measured in the full-scale facility. However, as the test-section dynamic pressure in the model is increased, the air-exchange rate falls off slightly to a level closer to that of the full-scale data. The model-scale data provided a reliable indication of the air-exchange performance of the full-scale system at the higher test-section dynamic pressures, which can be achieved in the full-scale tunnel.

With the model-scale wind tunnel, it was also possible to obtain a preliminary calibration of the air-exchange rate as a function of the position of the inlet door. The inlet door is hinged along its upstream edge and pivots out into the flow in the high-speed leg. The results of the calibrations are shown in Fig. 5. The air-exchange rate is shown plotted against the door opening expressed as a percent of the width of the north or high-speed leg of the wind tunnel circuit. Model-scale data were obtained both with and without an acoustic barrier installed near the air-exchange exhaust opening.[4] The barrier is intended to minimize radiation of noise into the surrounding community generated by models in the 40- by 80-ft test section. Also shown in the figure are two data points indicating the calibration of the full-scale inlet door position. The model- and full-scale results agree to within the experimental error.

The lateral distribution of total temperature in the test section was found to be quite similar in both facilities. A comparison was made of the lateral variation in total temperature as a percent of the differential between the internal and external ambient temperatures across the test sections of the model- and full-scale facility for the maximum air-exchange rate of 10%. The results are shown in Fig. 6. The error bars on the 1/50-scale data represent scatter in the small-scale measurements. The figure clearly shows a lower temperature on the inside of the circuit due to the location of the air-exchange inlet on the inside wall of the wind tunnel. The cool air admitted to the circuit from the courtyard area spirals toward the outside of the circuit in layers and is gradually warmed and mixed by the energy input from the fans. Warm air is expelled from the exhaust opening on the outside of the circuit downstream of the drive fans.

Total Pressure Surveys

A comparison of dynamic pressure surveys downstream of the air inlet door are presented in Fig. 7. The dynamic pressure

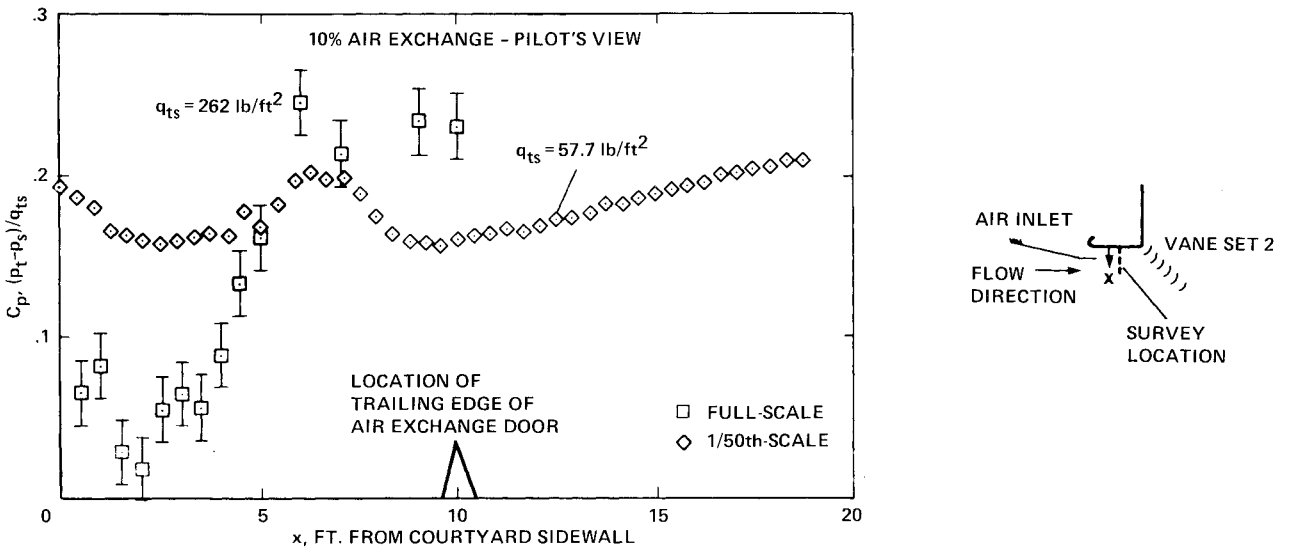

Fig. 7 Comparisons of dynamic pressure surveys downstream of air inlet door for full-scale opening corresponding to 10 ft.

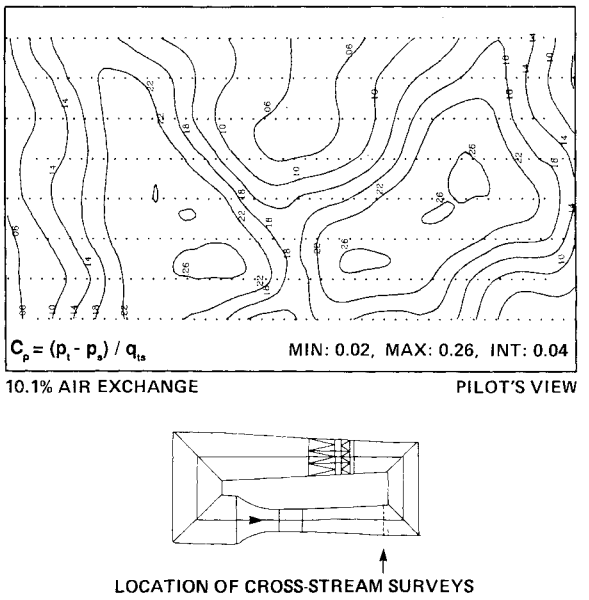

Fig. 8 Contour plot of dynamic pressure coefficients measured upstream of vane set 1 in 1/50-scale model.

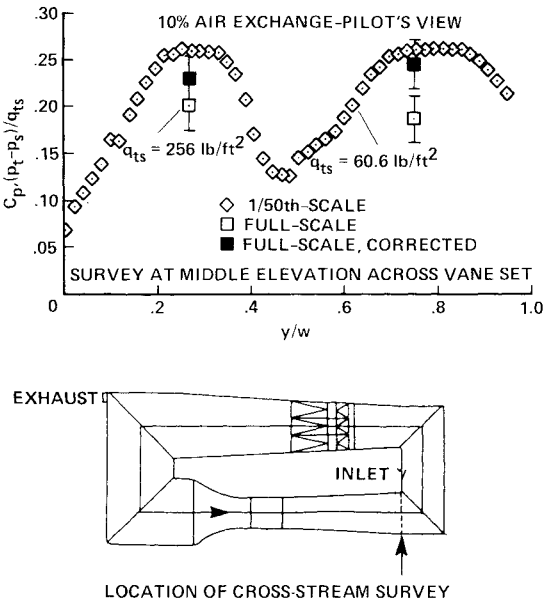

Fig. 9 Comparison of lateral distributions of dynamic pressure coefficients measured upstream of vane set 1.

as a function of the distance from the courtyard sidewall is shown for a 10% air exchange condition. Also shown in the figure is the relative lateral location of the trailing edge of the inlet door. The total pressure deficit in the core of the inlet flow near the wall evident in the full-scale data is greater than the 1/50-scale results indicate. A possible reason for this phenomenon is that the smooth, cylindrical intake cowling on the courtyard wall upstream of the full-scale inlet is penetrated at several vertical locations by large, wide-flange beams, which make up the external superstructure of the wind tunnel. Visualization of the full-scale inlet flow revealed that a portion of the total-pressure rake downstream of the inlet door was located in the wake of one of the exterior beams. It was not feasible to simulate the exterior structures accurately at small scale.

The configuration of the air inlet is intended to reduce separation and boundary-layer thickening downstream of the inlet and to produce a uniform velocity profile downstream of the inlet. In Fig. 7, the wake of the inlet door is less pronounced in the 1/50-scale data when compared with the full-scale results. This is probably because the model-scale surveys were performed at a scaled location, which was slightly farther downstream than that of the full-scale measurements. The full-scale measurements were obtained using a rake located 0.03 door chord lengths downstream of the trailing edge of the inlet door. The model-scale surveys were done 0.17 chord lengths downstream of the trailing edge.

In order to upgrade the speed capability of the full-scale wind tunnel complex, fan-drive power was increased by approximately a factor of four. The resulting speed and dynamic pressure increase at all locations in the circuit prompted a reanalysis of the design of existing structures within the wind tunnel. In some cases, the existing designs were found to be structurally inadequate. Among the aerodynamic features reanalyzed were the four sets of corner turning vanes.[8] Measurements of the total pressure upstream of a 1/50-scale model were used to provide estimates of the magnitude and distribution of the dynamic pressure upstream of the turning vanes. The results were then used to develop estimates of the aerodynamic loads to be used by the structural designers.

A typical contour plot of the dynamic pressure upstream of vane set 1 in the model is shown in Fig. 8. The dynamic pressure contours are nondimensionalized by test-section dynamic pressure. Two kidney-shaped lobes of high levels of dynamic pressure coefficient are evident to the left and right of the center. A region of reduced dynamic pressure is also evident near the center top of the plot. This particular distribution is caused by the presence of a streamwise row of structural support columns, which are oriented vertically along the centerline of the high-speed diffuser. Despite the fact that these columns are streamlined in cross section, a considerable wake is produced downstream. The flow on either side of the columns is unobstructed and retains more of its kinetic energy. Vortex generators located at the upstream end of the high-speed diffuser induce a clockwise swirl direction to the core flow on the left side of the diffuser and counterclockwise swirl to the flow on the right. This induced swirl pattern causes the distribution to be antisymmetric top to bottom.

With the model it was possible to obtain a relatively dense total pressure survey upstream of a particular vane set. For practical reasons, in the full-scale wind tunnel, the dynamic presure upstream of the vane sets was measured at relatively few locations. The Pitot-static probes used for the full-scale measurements were located in the areas expected to experience the highest levels of dynamic pressure based on the model-scale results. The full-scale data could then be used to verify the estimates of aerodynamic loading used for design purposes. Although the model-scale surveys required approximately 30 s to perform, time-dependent variations in the model-scale data were found to be small.

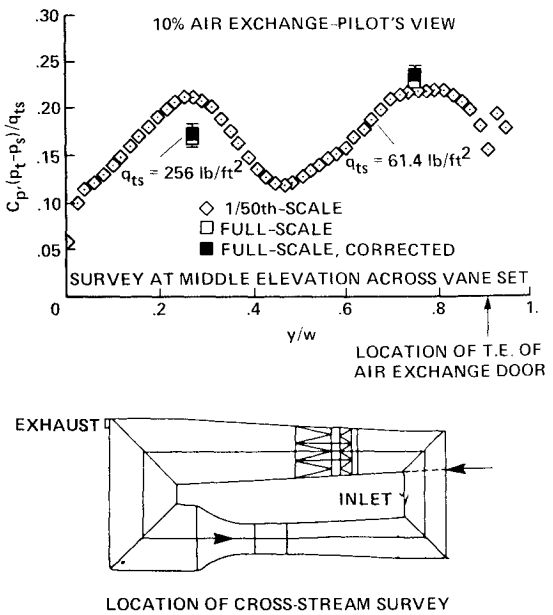

Fig. 10 Comparison of lateral distributions of dynamic pressure coefficients measured upstream of vane set 2.

Surveys in the model were performed at convenient locations upstream of the vane sets along lines perpendicular to the mean-flow direction. In contrast, the probes used to measure dynamic pressure upstream of the vane sets in the full-scale wind tunnel were situated approximately 1 chord length upstream of the leading edges of the vanes. Since the probes were located along a line parallel with the 45-deg stagger lein of the vane set, the probes were located farther downstream relative to the 1/50-scale survey location. The relative static pressure levels between the locations of the full- and model-scale measurements were different due to changes in area and the fact that the diffusion process upstream of the vane sets was not complete. For this reason, the full-scale dynamic pressure data were corrected to account for the difference in location between the model- and full-scale measurements. Detailed measurements of the streamwise distributions of static pressure upstream and downstream of the vane sets made in both the model- and full-scale wind tunnels enabled the magnitude of the corrections to be estimated.

A comparison of the dynamic pressure levels of the flow upsteam of vane set 1 in the model- and full-scale wind tunnels is presented in Fig. 9. The survey line is located along the horizontal centerline of the vane set. Both corrected and uncorrected full-scale data are presented along with the results from the model scale survey. Data are presented for a test-section dynamic pressure of 60.6 lb/ft^2 in the model and 256 lb/ft^2 in the full-scale facility. The wake of the diffuser support columns is clearly visible in the center. The core regions of high velocity flow are evident on each side. When the full-scale dynamic-pressure coefficients are corrected for the offset in static pressure, the agreement with the model-scale results is nearly within the scatter band of the full-scale data.

A similar comparison of the dynamic-pressure coefficients measured upstream of vane set 2 is shown in Fig. 10. Data are presented for test-section dynamic pressures of 61.4 lb/ft^2 in the model and 256 lb/ft^2 in the full-scale facility. The wake of the support columns in the primary diffuser and the high-velocity regions are still evident at this section. The wall jet due

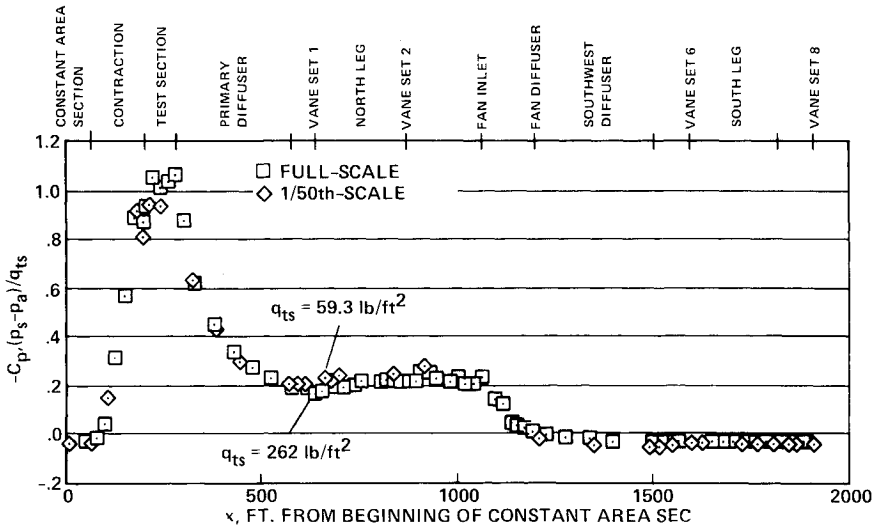

Fig. 11 Comparison of distributions of static pressure coefficients measured along ceiling centerline of 1/50- and full-scale wing tunnels.

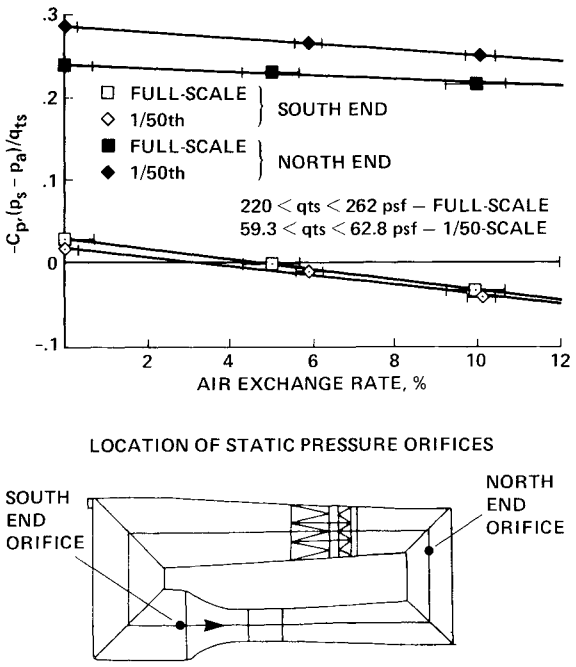

Fig. 12 Comparison of static pressure coefficients measured in high- and low-speed legs of 1/50- and full-scale wind tunnels.

to the air-exchange inlet located directly upstream of the vane set can also be seen in the 1/50-scale survey on the right side of the figure. Because the high-speed leg of the wind-tunnel upstream of vane set 2 is a constant area duct, the static pressure correction to the full-scale measurements of dynamic pressure at the vane set is much smaller than that used for the vane set 1 data.

Circuit Pressure Distribution

A comparison of the differential wall pressure coefficients for the full-scale and 1/50-scale wind tunnels at an air-exchange rate of 10% is shown in Fig. 11. The pressure coefficients are plotted along the flow direction beginning at the constant-area sections or settling chambers of the two tunnels. Also shown across the top of the figure are the locations of the major elements comprising the wind-tunnel circuit. Good agreement is noted between the full-scale and model-scale data over the entire length of the circuit. The minor differences between the static pressure levels in the two tunnels are evident in the test-section area and in the north end of the circuit. These differences can be attributed to minor geometrical differences between the two tunnels, to higher drag of the model-scale turning vanes due to Reynolds number effects, and to the fact that an instrumentation boom with flow-quality sensors was present in the test section of the full-scale tunnel when the circuit pressure data were acquired. The blockage in the full-scale test section of the wind tunnel may account for the elevated suction pressures there. No sensors were present in the test section of the model when the model-scale data were acquired. The static pressure levels in the south end of the two tunnels are nearly identical because both circuits are vented to atmospheric pressure by the relatively large air exhaust openings located at the southwest corner.

One measure of the performance of a wind tunnel is the pressure balance between the high-speed section upstream of the fan drive and the low-speed or settling chamber area of the circuit. The pressure balance provides an indication of the overall pressure losses within the circuit including the drag of the turning vane sets and the pressure rise of the fans. The data in Fig. 12 show a comparison of the pressure levels within the high- and low-speed legs of the model- and full-scale tunnels nondimensionalized by test-section dynamic pressure as a function of the air-exchange rate. The locations of the orifices at which the pressures were measured are indicated on the diagram of the wind tunnel. In the high-speed leg, the suction pressures in the 1/50-scale facility are approximately 10% greater than in the full-scale wind tunnel. This is probably due to the greater drag of the model-scale turning vane sets relative to their full-scale drive fans. As the air-exchange rate is increased, the pressure level within the two facilities increases linearly (shown as a negative slope on the plot). This is due to an increased venting of the north end of the circuit where the air inlet is located. As the air-exchange rate is increased, the pressure in the south end changes sign from negative at 0% air exchange to positive at 10% air exchange.

Concluding Remarks

A 1/50-scale model of the NFAC 40- by 80-ft wind tunnel has been used in performance and design studies of various modifications to the full-scale facility. Model-scale measurements of test-section flow quality, air-exchange rate, and total and static pressure distributions have been compared with results of the full-scale Integrated Systems Test. Despite the large differences in scale and Reynolds number between the two facilities, qualitative performance trends of the full-scale facility were well simulated by the model wind tunnel. In general, the quantitative agreement of the data from the two facilities was quite good. It has been demonstrated that a small-scale wind-tunnel model can be used successfully for aerodynamic design and performance verification of a very large-scale, closed-circuit wind tunnel.

References

[1]Corsiglia, V. R., Olson, L. E., and Falarski, M. D., "Aerodynamics Characteristics of the 40- by 80/80- by 120-Foot Wind Tunnel at Ames Research Center," NASA TM 85946, 1984.

[2]Page, V. R., Eckert, W. T., and Mort, K. W., "An Aerodynamic Investigation of Two 1.83-Meter-Diameter Fan Systems Designed to Drive a Subsonic Wind Tunnel," NASA TM 73175, 1987.

[3]Schmidt, G. I., Rossow, V. J., van Aken, J., and Parrish, C. J., "One-Fiftieth Scale Model Studies of the 40- by 80-Foot and 80- by 120-Foot Wind Tunnel Complex at NASA Ames Research Center," NASA TM 89405, 1987.

[4]Smith, B. E. and Naumowicz, T., "Aerodynamic Characteristics of the Modified 40- by 80-Foot Wind Tunnel as Measured in a 1/50th-Scale Model," NASA TM 88336, 1987.

[5]Perry, A. E., *Hot Wire Anemometry*, Oxford University Press, New York, 1982, Chap. 8.

[6]Rossow, V. J., Schmidt, G. I., Meyn, L. R., and Holmes, R. E., "Aerodynamic Characteristics of an Air-Exchanger System for the 40- by 80-Foot Wind Tunnel at Ames Research Center, NASA TM 88192, 1986.

[7]Olson, L. E., Zell, P. T., Soderman, P. T., Falarski, M. D., Corsiglia, V. R., and Edenborough, H. K., "Aerodynamic Flow Quality and Acoustic Characteristics of the 40- by 80-Foot Test Section of the National Full-Scale Aerodynamics Complex," Society of Automotive Engineers, Warrendale, PA, SAE Tech Paper 872328, 1987.

[8]Aoyagi, K., Olson, L. E., Peterson, R. L., Yamauchi, G. K., Ross, J. C., and Norman, T. T., "Time-Averaged Aerodynamic Loads of the Vane Sets of the 40- by 80-Foot and 80- by 120-Foot Wind Tunnel Complex," NASA TM 89413, 1987.